SUPPLEMENTARY MATERIAL

Non-purified commercial multiwalled carbon nanotubes supported on electrospun polyacrylonitrile@polypyrrole nanofibers as photocatalysts for water decontamination

Capilli Gabriele[a,1], Damian Rodríguez Sartori[b], Monica C. Gonzalez[b], Enzo Laurenti[a], Minero Claudio[a], Paola Calza[a,*]

[a] Dipartimento di Chimica, Università degli Studi di Torino, via Pietro Giuria 5/7 – 10125 Torino, Italy

[b] Instituto de Investigaciones Fisicoquímicas Teoricas y Aplicadas (INIFTA), CCT-La Plata-CONICET, Universidad Nacional de La Plata, Diagonal 113 y 64, La Plata, Argentina

[1] Present address: Mining & Materials Engineering, McGill University, 3610 University Street, Montreal, Quebec H3A 0C5, Canada

[*] Corresponding author. E-mail address: paola.calza@unito.it

Table of contents

This document provides supporting information on some of the methods used to synthesize the composite structure and details and results not presented in the main text.

1. Materials and Methods

1.1. Electrospinning conditions for PAN nanofibers

We selected a solution of PAN in DMF at concentration of 20% w/w, after testing a range of concentration between 12% and 25%. The 20% solution was best for electrospinning: at lower concentrations, some beads were present in the fibers, while at higher concentrations the solvent was evaporating too fast during electrospinning. The optimized conditions to obtain uninterrupted electrospun fibers were: relative humidity = 40-48%, temperature = 22-25 °C, applied voltage = 16 kV, needle-collector distance = 20 cm, flux = 0.8-0.65 ml h^{-1}. We collected the PAN nanofibers on a plane collector, covered with aluminum foil.
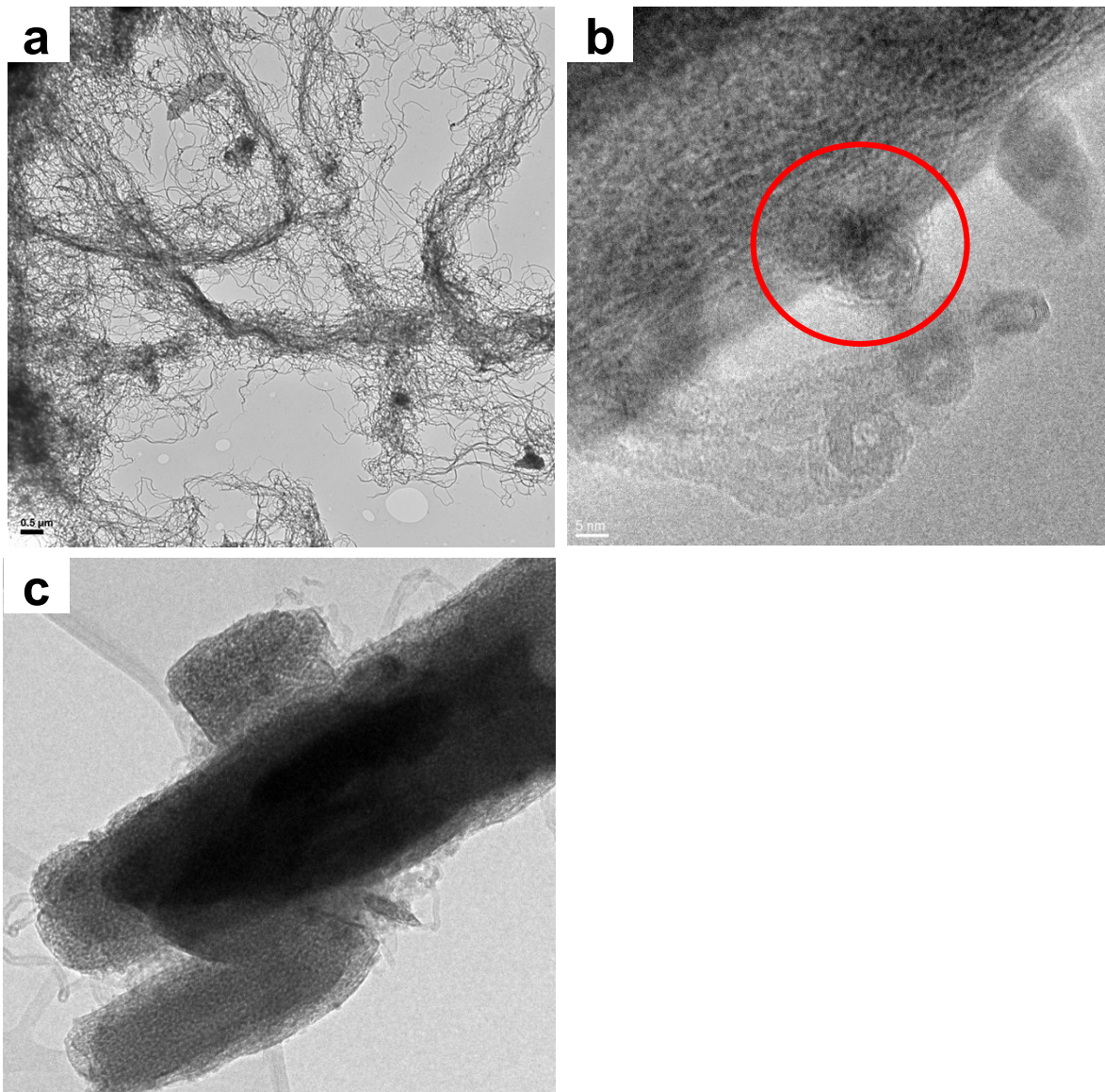
2. Results

2.1. TEM

Figure S1. (a) TEM micrography of non-purified commercial multiwalled carbon nanotubes CNT(NP), **(b)** HRTEM micrography of a CNT(NP) with a metal oxide nanoparticle embedded in the nanotube structure, highlighted by the red circle, **(c)** HRTEM micrography of a CNT(NP) showing its multi-walled structure.
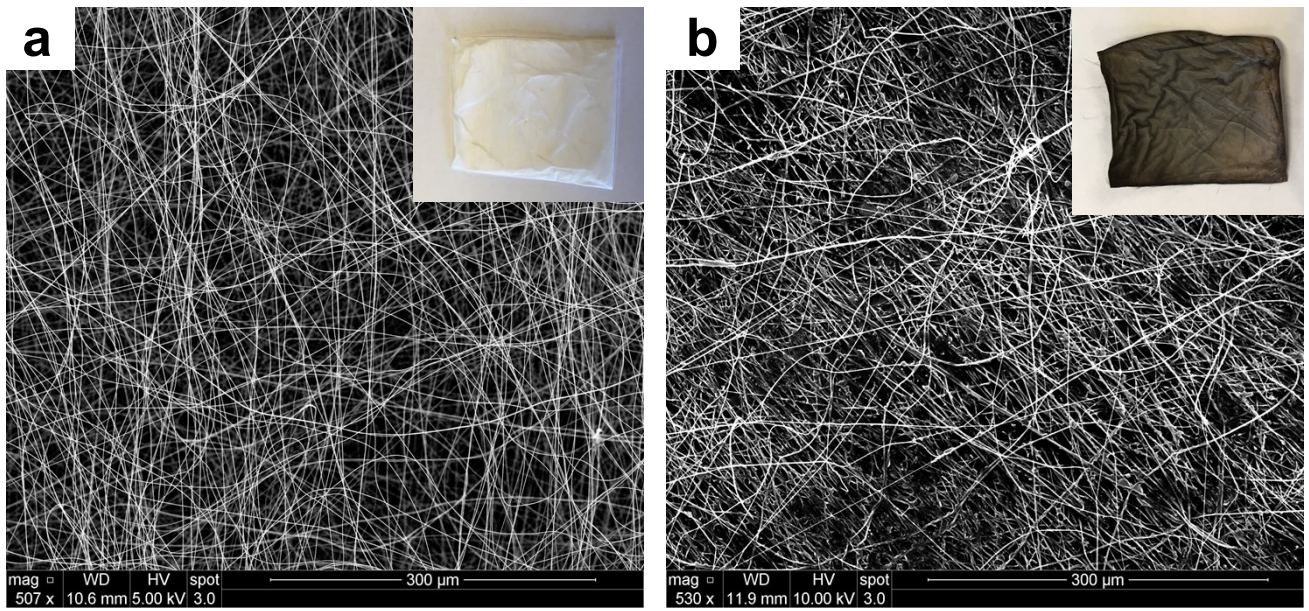
2.2. SEM

Figure S2. SEM micrographs of (a) PAN nanofibers and (b) PAN nanofibers after 3 depositions cycles of PPY.
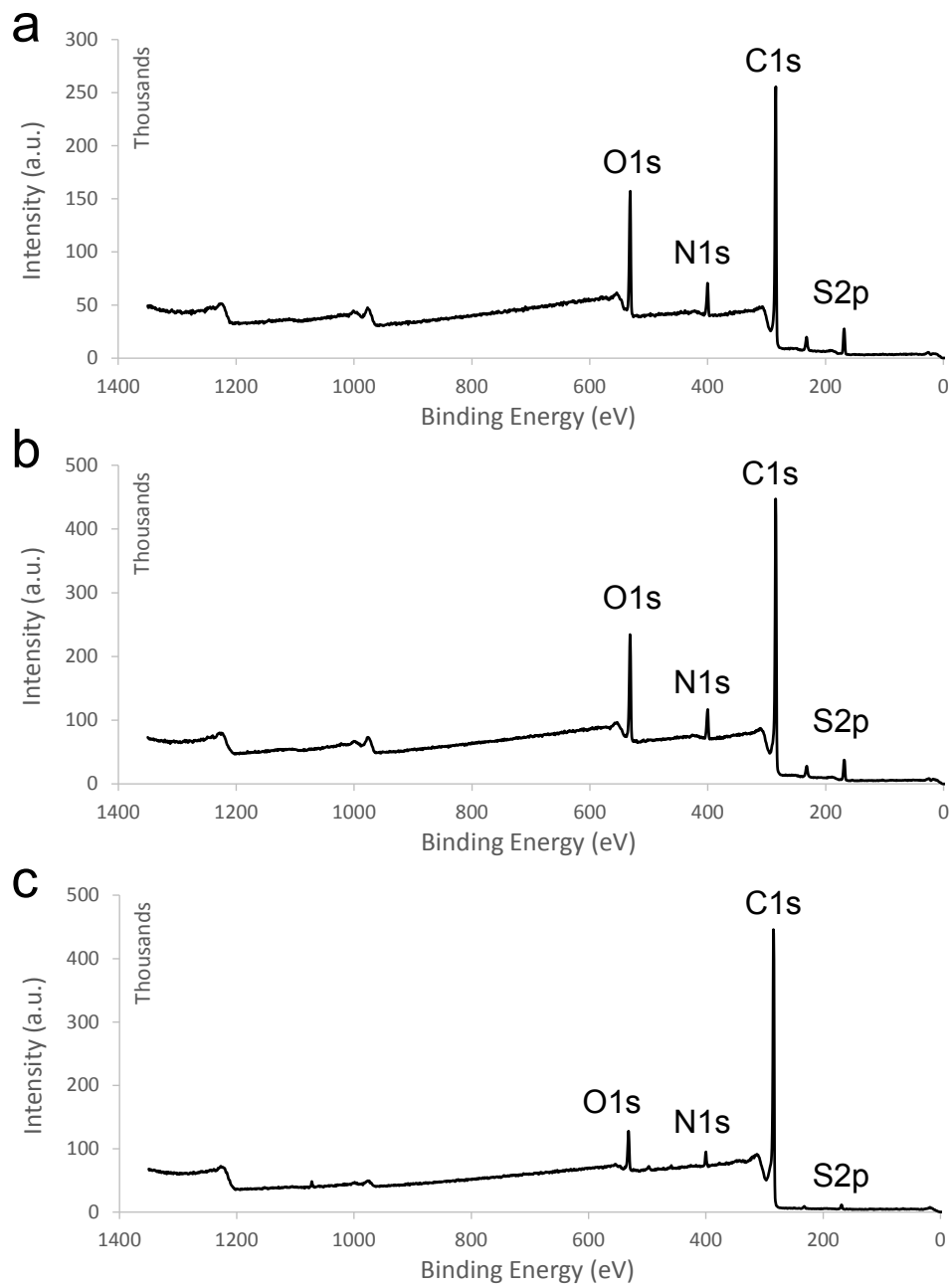
2.3. XPS

Figure S3. XPS survey scans of a PAN@PPY mat (a), the spot of the PAN@PPY-CNT(NP) composite with the lowest amount of CNT(NP) deposited (b), and the spot of the PAN@PPY-CNT(NP) composite with the highest amount of CNT(NP) deposited (c).
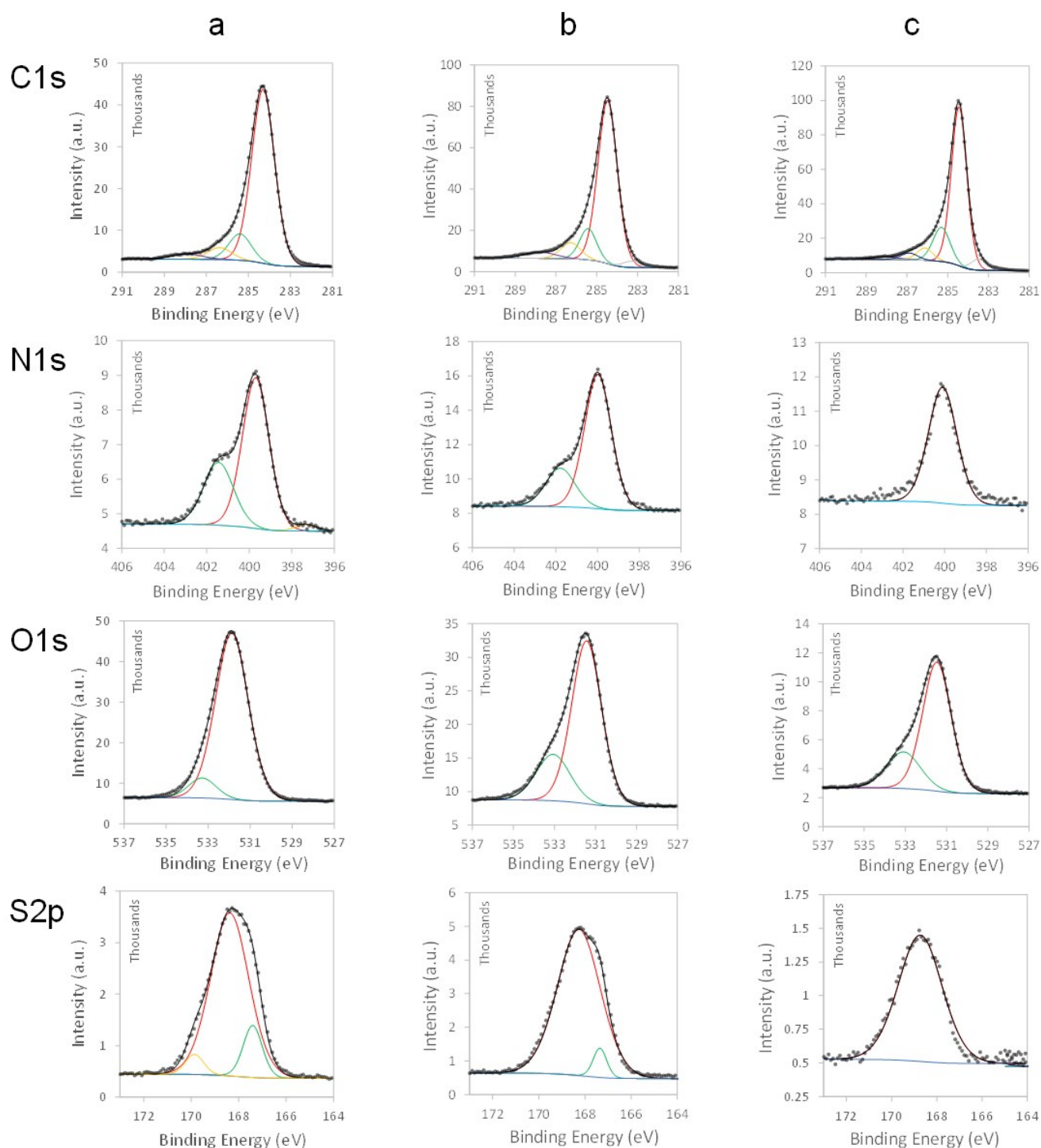
Figure S4. High resolution XPS deconvoluted spectra of C, N, O, and S for PAN@PPY mat (a), PAN@PPY-CNT(NP) composite (b), and the spots of the PAN@PPY-CNT(NP) composite with a higher amount of CNT(NP) deposited on the surface (c). Experimental data is shown as grey dots, individual fitting components are in color and the overall fit in black solid line.

The high-resolution C 1s XPS spectra of PAN@PPY and PAN@PPY-CNT(NP) samples reveal 4 to 6 components, two of which probably result from the contribute of different species with chemical shifts too close to be deconvoluted with the instrumental resolution. In all the samples the main peak

corresponds to C sp^2 (~284.3 eV, red fit), typical of the aromatic pyrrole rings, followed by that of C–N$^+$ / C–N (~285.4 eV, green fit), C=N$^+$ / C=N / C–O (~286.4 eV, yellow fit), and the π-π* shake up (~288.0 eV, purple fit).[1,2] Comparison of the XPS spectra in the C 1s region shows, in the case of PAN@PPY-CNT(NP) samples, the increase of the contribution at ~286.4 eV and/or the appearance of a signal at ~287.0 eV, attributed to C=O, which are probably correlated to a higher amount of exposed C–OH / –COOH groups. The increase of surface carbonyl groups is also observed in the O 1s spectra (532-533 eV).

The deconvolution of the highly resolved N 1s region shows two main components. The signal at ~400 eV (red fit) is readily assignable to the –NH– group of the pyrrole units, while that at 401.8 eV corresponds to the bipolaron C=N$^+$ structure (with partial contribution of polarons, C–N$^+$, usually reported at ~401 eV).[1,2] The little signal at ~398 eV corresponds to C=N (iminic nitrogen) impurities. The S/N atomic ratio, as determined by XPS, allows to evaluate PPY doping. Alternatively, the N$^+$/N ratio, calculated from the components of the deconvoluted N 1s band, usually gives similar results.[1,2] These two values correspond approximately to 0.4 and 0.3 in the case of PAN@PPY. This implies that the oxidative polymerization generates a very pronounced doping level (higher than 1 pyrrole ring every 3), which is kept stable by the DBS anion incorporation into the PPY structure.[1] The N$^+$/S ratio close 1 implies that the positive charges are mostly located on N centers.

The high resolution XPS O 1s spectrum show that oxygen is located almost entirely in the sulfone heads of DBSA anions, in the form of S=O (531.5 eV, red fit). This agrees with the S 2p spectrum which shows a predominance of highly oxidized sulfur, i.e. sulphate/sulfone groups (~168.5 eV, red peak fit). After functionalization with nanotubes, the O 1s spectrum shows an increase of C–OH surface moieties (~533.0 eV, green peak fit), probably localized on the exposed nanotube surface, not completely coated with the PPY layer.
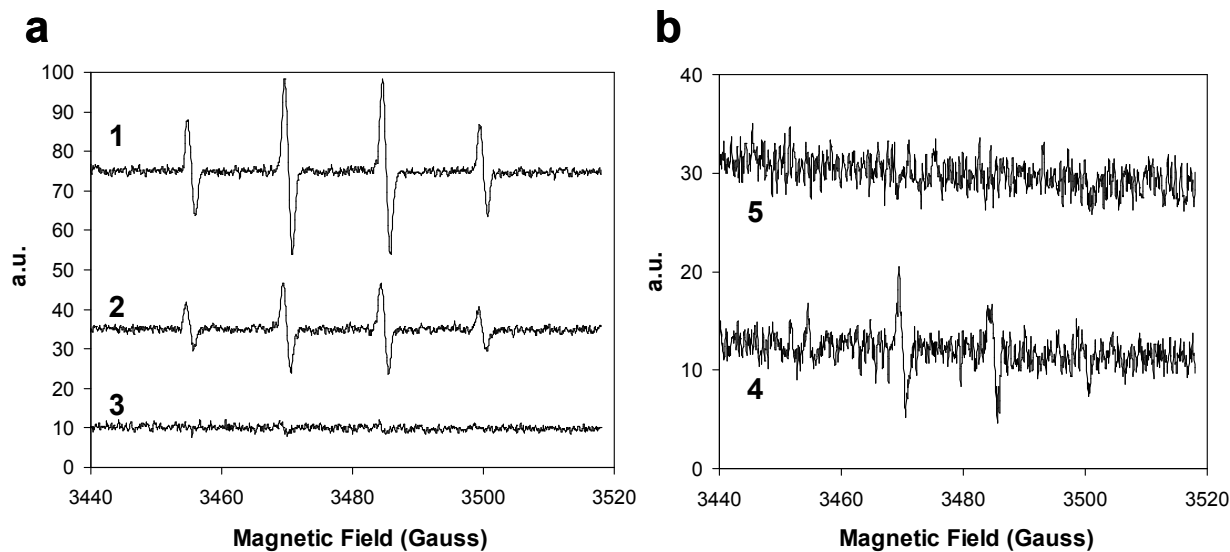
2.4. EPR

Figure S5. (a) EPR spectra of 1) electrospun PAN nanofibers, 2) PAN-CNT(NP) nanofibers, 3) PAN@PPY nanofibers. (b) EPR spectra of 4) 10 ppm suspension of pristine CNT(NP), 5) 10 ppm suspension of CNT (CNT(NP) after treatment with conc. HCl).

The high signal recorded in the EPR spectrum of PAN (1) is probably due to the presence of residual radical initiators used to polymerize the acrylonitrile units. Spectrum 2) shows how CNT(NP) exhibit a quenching activity toward the radicals produced from the irradiation of PAN. Spectrum 3) reveals that in PAN@PPY nanofibers the extinction of •OH radicals production is due to the PPY sheath which shields the incoming light. A comparison between the EPR spectra of water suspended CNT(NP) and CNT (4 and 5) demonstrates that just CNT(NP) are capable of photogenerating •OH radicals. Then, the HCl-based cleaning step described in the main article (section 2.2.4) removes the photoactive metal/metal oxide NP embedded in the non-purified carbon nanotubes.
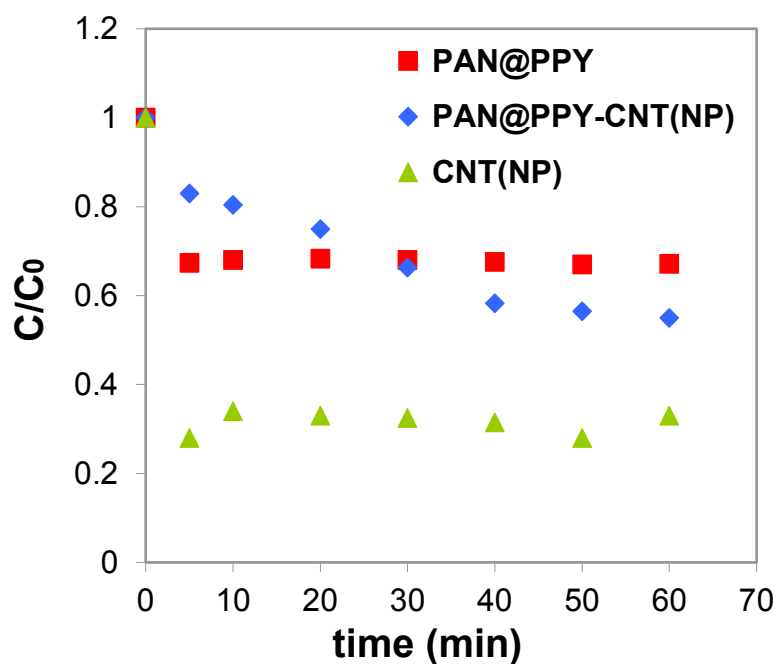
2.5. RB adsorption

Figure S6. Adsorption of Rhodamine B on PAN@PPY (■), PAN@PPY-CNT(NP) (♦), and a 50 ppm water dispersion of pristine CNT(NP) (▲).

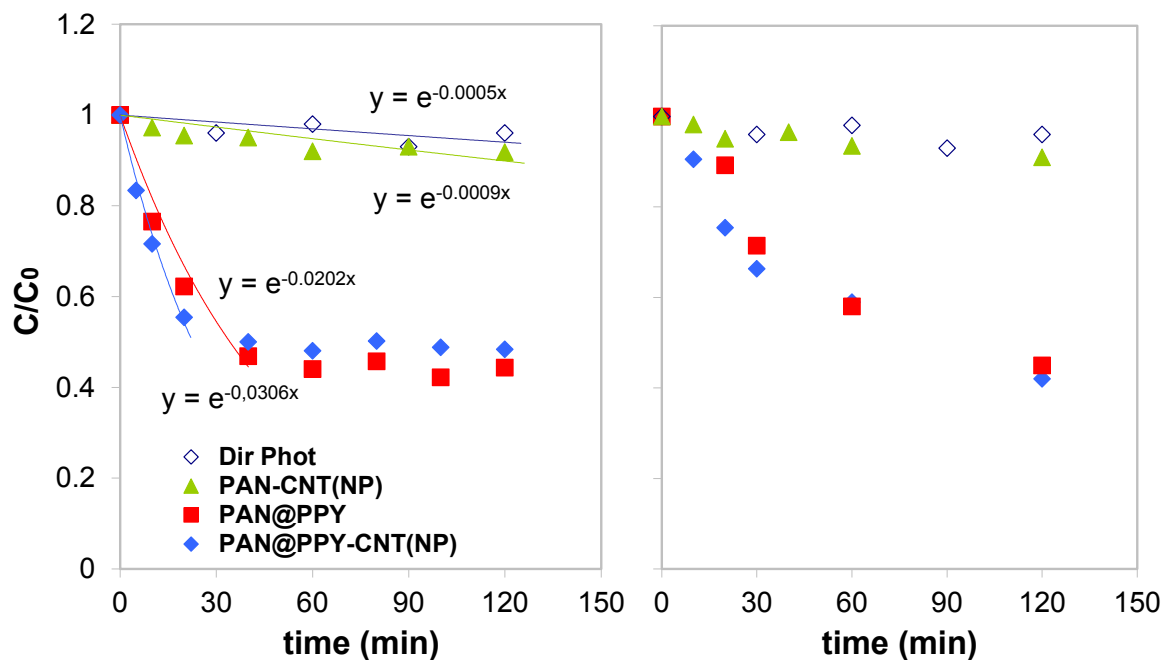## 2.6. Naphthalene photodegradation

Figure S7. The first two removal cycles for naphthalene (5 ppm in water), carried out using PAN-CNT(NP) (▲), PAN@PPY (■) and PAN@PPY-CNT(NP) (♦) mats under Solarbox irradiation. The direct photolysis of naphthalene (◊) is also reported.

2.7. TOC

Irradiation time (min)	mg of carbon released per cm^2 of the mat		
	PAN-CNT(NP)	PAN@PPY	PAN@PNP-CNT(NP)
0	0.01	0.11	0.08
15	0.02	0.20	0.14
30	0.01	0.21	0.15
60	0.01	0.21	0.16
120	0.02	0.21	0.15

Table S1. Total organic carbon (TOC) released by PAN-CNT(NP), PAN@PPY, and PAN@PPY-CNT(NP) mats exposed to UV-Vis irradiation for different time frames. The error in the experiment is of 0.01 mg C release cm^{-2} mat.

2.8. Tensile tests

Sample	Thickness (µm)	Ultimate Tensile Strength (MPa)	Elongation at break (%)	Young's modulus (MPa)
PAN@PPY-CNT(NP)	30 ± 10	10 ± 3	50 ± 15	200 ± 70
PAN@PPY-CNT(NP) after 1-week irradiation	45 ± 10	6 ± 2	30 ± 8	90 ± 30

Table S2. Summary of 3 important mechanical parameters of PAN@PPY-CNT(NP) mats, before and after prolonged irradiation, calculated from the stress-strain plots in Figure 6 of the main article.

The tensile strength and Young's modulus of our composite mats are comparable to that of other reported electrospun PAN nanofibers.[3] In literature much higher values are present, but they mostly correspond to measurements carried out on single electrospun nanofibers or highly oriented/interwoven mats.[4] It must also be noted that the Young's moduli and ultimate strengths present in Table S2 are underestimations of the actual values, since part of the mat thickness is just composed of PPY and nanotubes which do not contribute substantially to the mechanical properties of the mat. Moreover, the wide standard deviation reported for the Young's moduli are mainly due to the intrinsic uncertainty in the measurement of the mat thickness, which have a relevant effect on the calculation of the cross sections.

3.   References

1) J. Tabačiarová, M. Mičušík, P. Fedorko, M. Omastová, Study of polypyrrole aging by XPS, FTIR and conductivity measurements, *Polym. Degrad. Stab.,* **2015** (120) 392.

2) C. Malitesta, I. Losito, L. Sabbatini, P. G. Zambonin, New findings on polypyrrole chemical structure by XPS coupled to chemical derivatization labelling, *J. Electron. Spectros. Relat. Phenomena*, **1995** (76) 629.

3) S. A. Karim, A. Mohamed, M. M. Abdel-Mottaleb, T. A. Osman, A. Khattab, Mechanical Properties and the Characterization of Polyacrylonitrile/Carbon Nanotube Composite Nanofiber, *Arab. J. Sci. Eng.,* **2018** (43) 4697.

4) J. Yao, C. W. M. Bastiaansen, T. Peijs, High Strength and High Modulus Electrospun Nanofibers, *Fibers,* **2014** (2) 158.